

Final Scientific/Technical Report

REPORT NUMBER DOE-UTEXAS-0000841

Models and Strategies for Optimal Demand Side Management in the Chemical Industries

WORK PERFORMED UNDER AGREEMENT

DE-OE0000841

The University of Texas at Austin
1 University Station
Austin, TX 78712

Award Period of Performance: August 2016 to January 2020

Submitted: April 27, 2020

PRINCIPAL INVESTIGATOR

Michael Baldea

TEAM MEMBERS

Ross Baldick

SPONSORING PROGRAM OFFICE

U. S. Department of Energy
Office of Electricity Delivery and Energy Reliability
Via the National Energy Technology Laboratory

TABLE OF CONTENTS

<i>LIST OF TABLES</i>	3
<i>LIST OF FIGURES</i>	4
<i>LIST OF ACRONYMS AND ABBREVIATIONS</i>	5
<i>I. Executive Summary</i>	6
<i>II. Objectives</i>	7
<i>III. Technical Approach</i>	9
<i>IV. Accomplishments and Conclusions</i>	26
<i>APPENDIX A: Product or Technology Production</i>	27
<i>REFERENCES</i>	29

This material is based upon work supported by the Department of Energy under Award Number(s) DE-OE0000841.

This report was prepared as an account of work sponsored by an agency of the United States Government. Neither the United States Government nor any agency thereof, nor any of their employees, makes any warranty, express or implied, or assumes any legal liability or responsibility for the accuracy, completeness, or usefulness of any information, apparatus, product, or process disclosed, or represents that its use would not infringe privately owned rights. Reference herein to any specific commercial product, process, or service by trade name, trademark, manufacturer, or otherwise does not necessarily constitute or imply its endorsement, recommendation, or favoring by the United States Government or any agency thereof. The views and opinions of authors expressed herein do not necessarily state or reflect those of the United States Government or any agency thereof.

LIST OF TABLES

Table 1: Summary of scheduling-relevant variables and their rationale, from [5].....	11
Table 2: Summary of model fits for the HW models from [5].....	13
Table 3: Summary of model fits for the FSR models from [5].....	13
Table 4: Model statistics for linearized HW models.	13
Table 5: Summary of results for the 3-day DR scheduling problem of an ASU when optimal schedules for DR2-DR5 were simulated on the full-order model of the ASU. *ROC solution had several constraint violations [5].....	16

LIST OF FIGURES

Figure 1: 3-day electricity price and renewables availability for July 3-5, 2017 provided by CAISO [1], [2].	7
Figure 2: Process flow diagram for the industrial ASU used to generate preliminary operating data, based on Johannsson [4].	9
Figure 3: Historical data from industrial process and preliminary data-driven model predictions from [6].	10
Figure 5: Hierarchy of decisions for chemical process operation, where u are the production set-points/targets and w are the values of the process variables.....	12
Figure 6: HW model form, from [5].	12
Figure 7: Problem structure for DR3.	16
Figure 8: 3-day emissions and operating cost for EMP, DR, and the reference problem (without DR) from [8].	18
Figure 9: Histogram of the simulated operating cost across all scenarios for CC1-CC2 and the reference problem (no DR), with labeled vertical lines representing the mean values from [9]..	20
Figure 10: Histogram of the simulated operating cost across all scenarios for CC1, CC4, and the reference problem (no DR), with labeled vertical lines representing the mean values from [9]..	21
Figure 11: Energy benefit for the next time horizon, where a negative benefit signifies depleted storage, from [9].....	21
Figure 12: Scheduling schemes for periodic (daily) pricing updates, where three scheduling methods are considered, from [10].	22
Figure 13: Scheduling schemes for periodic (every 6 hours) temperature updates, where three scheduling methods are considered, from [10].	23
Figure 14: Scheduling schemes for event-driven rescheduling.	24

LIST OF ACRONYMS AND ABBREVIATIONS

Air Separation Unit (ASU)
Demand Response (DR)
Dispatchable DR (DDR)
Distributed Resource Energy and Ancillaries Market (DREAM)
Emissions-Minimizing Production (EMP)
Finite Step Response (FSR)
Hammerstein Wiener (HW)
Lagrangian Relaxation (LR)
Moving-Horizon (MH)
Non-Dispatchable DR (NDDR)
Parts-Per-Million (ppm)
Primary multi-stream heat exchanger (PHX)
Rate of Change (ROC)
Scale-Bridging Model (SBM)
Security-Constrained Economic Dispatch (SCED)
Special Ordered Sets of Type II (SOS2)

I. Executive Summary

Deregulation and the increase of renewable electricity generation from wind and solar photovoltaics have transformed the U.S. electricity market. Economic and environmental benefits notwithstanding, the presence of renewables has increased variability and uncertainty on the supply side of the grid. Managing demand, rather than generation – a strategy referred to as “demand response (DR)” – is an attractive approach for mitigating this imbalance. DR efforts aim to reduce electricity usage during peak demand times, lessening stress on the grid. Industrial users are particularly attractive entities for DR participation since they present large, localized loads that can provide significant relief on grid demand and –unlike other large loads, such as buildings – are minimally dependent on human needs and preferences.

In this project, we accomplished three main objectives.

1. We developed data-driven low-order DR scheduling-relevant dynamic models of chemical processes. Concurrently, we studied the formulation and solution of the associated optimal DR production scheduling problems.
 - a. A prototype air separation unit (ASU) model was used to generate simulated operating data for initial modeling efforts, which enabled the later use of industrial data for data-driven modeling.
 - b. We utilized Hammerstein-Wiener (HW) and Finite Step Response (FSR) models to represent nonlinear plant dynamics.
 - c. The HW models were linearized using exact linearization so they could potentially be embedded in power system models, which are formulated as mixed integer linear programs (MILPs)
 - d. We solved DR optimization problems under uncertainty and found that even naïve predictions of electricity price and product demand led to significant cost savings benefits.
2. Our DR scheduling optimization problem formulations are amenable to real-time solution.
 - a. We utilized Lagrangian Relaxation (LR) to efficiently solve the optimization problem by decoupling subproblems linked by complicating constraints.
 - b. We have achieved computation times for the 3-day DR scheduling problem of an ASU as low as 1.88 minutes [1].
3. Our representations of the DR behavior of chemical process as grid-level batteries were embedded in power system models.
 - a. For a small-scale grid, we found that incorporating the dynamics of the chemical plant in the optimal power flow calculations resulted in better resource management leading to up to 15% and 46% cost reduction for the grid and chemical plant operations, respectively, during periods of power line congestion.

We have published several works dedicated to modeling and solving DR optimization problems from the user side. These were published in top peer-reviewed journals and are summarized in this report. The most recent work (and papers in preparation) considers DR scheduling from the grid side. Future efforts will consider networked plants (e.g., air separation units operating on a common pipeline) for DR participation, which is expected to amplify the capabilities of industrial DR participants to perform load-shifting. Our consideration of uncertainty in DR has inspired future directions in this area as well: we plan to develop multistage methods to fully account for the effects of uncertainty in DR scheduling.

II. Objectives

Deregulation and the increase of renewable electricity generation from wind and solar photovoltaics have transformed the U.S. electricity market. Economic and environmental benefits notwithstanding, the presence of renewables (Figure 1) has increased variability and uncertainty on the supply side of the grid. Managing demand, rather than generation – a strategy referred to as DR (demand response) is an attractive approach for mitigating this imbalance. DR efforts aim to reduce electricity usage during peak demand times, lessening stress on the grid. Industrial users are particularly attractive for DR participation since they present large, localized loads that can provide significant relief on grid demand and are minimally dependent on human needs such as air conditioning, enabling more flexible power demand. Under DR operation, an industrial site increases production during off-peak hours, storing product in excess of demand and later using this product to meet demand during peak grid power demand times, when production level at the industrial site is lowered. Such a scheme effectively amounts to storing energy in the form of a physical product. Thus, in order to participate in DR, an industrial site must not be able to store product safely and efficiently, as well as being able to modulate production rate on the same timescale as electricity price changes.

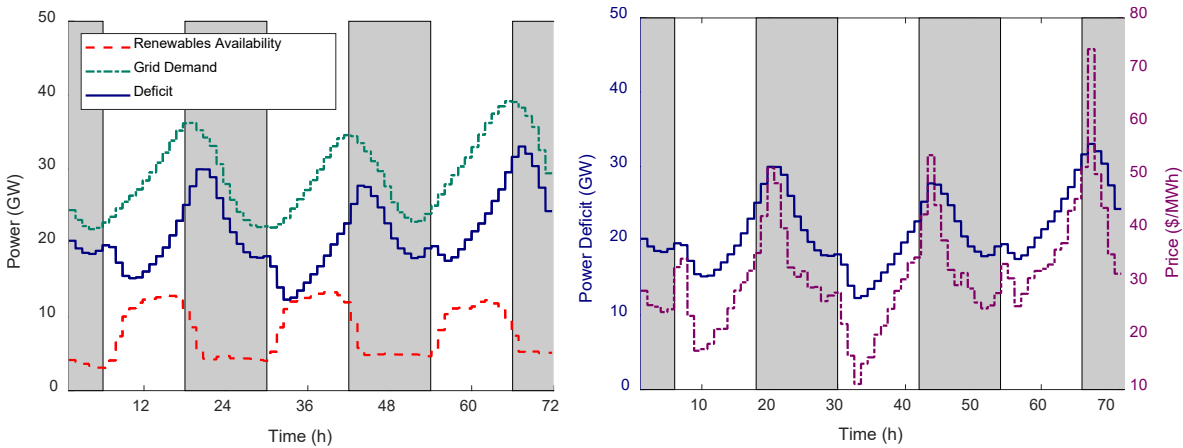


Figure 1: 3-day electricity price and renewables availability for July 3-5, 2017 provided by CAISO [3], [4].

The production modulation strategy outlined above can be imposed via judicious production scheduling. Changes in electricity prices can occur at different frequencies, ranging from every several hours (Figure 1) to, in some cases, every 5 minutes [5]. These changes are on the same timescale as the dynamics of typical key variables in an industrial plant of the kind considered in this project (i.e., electricity-intensive chemical plants), and therefore, it becomes necessary to embed dynamic process models into DR production scheduling calculations to ensure that scheduling moves account for the relevant dynamic behavior. Embedding information on process dynamics and control in scheduling calculations is challenging: for industrial processes, dynamic models are typically large-scale, nonlinear, and stiff, making the resulting optimization problems difficult to solve.

Motivated by the above, in this project, we aim to accomplish the following objectives:

1. Develop data-driven low-order, DR scheduling-relevant dynamic models of chemical processes:

Utilize historical operating data (augmented by a limited number of experimental tests) to derive low-order models of the nonlinear dynamics of chemical plants that are relevant to scheduling their operation for participating in DR programs. Concurrently, the formulation and solution of the associated optimal DR production scheduling problems was studied.

2. Develop DR scheduling optimization problem formulations that are amenable to real-time solution.

Develop a novel, feedback-based DR scheduling paradigm, and consider optimizing process operations from a grid-centric or process-centric perspective, allowing for DDR (dispatchable DR) for grid stability and improving process economics via NDDR (non-dispatchable DR).

3. Create representations of the DR behavior of chemical process that can be embedded in power system models.

Devise new pricing and bilateral coordination mechanisms to encourage NDDR behaviors that are optimal from a grid perspective.

The proposed research has led to generic tools and methodologies that are applicable to all manufacturing facilities in the chemical and petrochemical sector and can be extended to other industries. We **applied and validated** our findings by collaborating with an industrial partner from the energy-intensive air separation sector. In addition to the benefits provided to the grid, our preliminary results suggest that engaging in DR programs can save up to 3% of operating cost in this sector, compared to operating at a constant production rate with fixed energy prices. Significant additional income can be generated from providing ancillary services, such as responsive reserve. In discussing our approach to completing the project tasks, we will refer to two air separation case studies (industrial plant and a model of a prototype air separation plant) to illustrate the concepts that we developed.

III. Technical Approach

Task 1.0 Update Project Management Plan (PMP)

The Recipient updated the PMP to reflect how the project was managed. The PMP followed the template provided by DOE in the Funding Opportunity Announcement (FOA).

Task 2.0 Data Collection

Task 2.1 Simulation data collection

We considered an air separation unit (ASU) as a prototype electricity-intensive chemical plant. A simulation model of an ASU previously developed in our group [6] was used to generate a preliminary data set covering the transition of the chemical plant between different production rates. The data set contains information relating power demand to the production rate of nitrogen, as well as information concerning relevant plant variables (e.g., product purity, temperatures and pressures in different locations in the plant where sensors are available in practice, etc.). A process flow diagram of the ASU is in Figure 2.

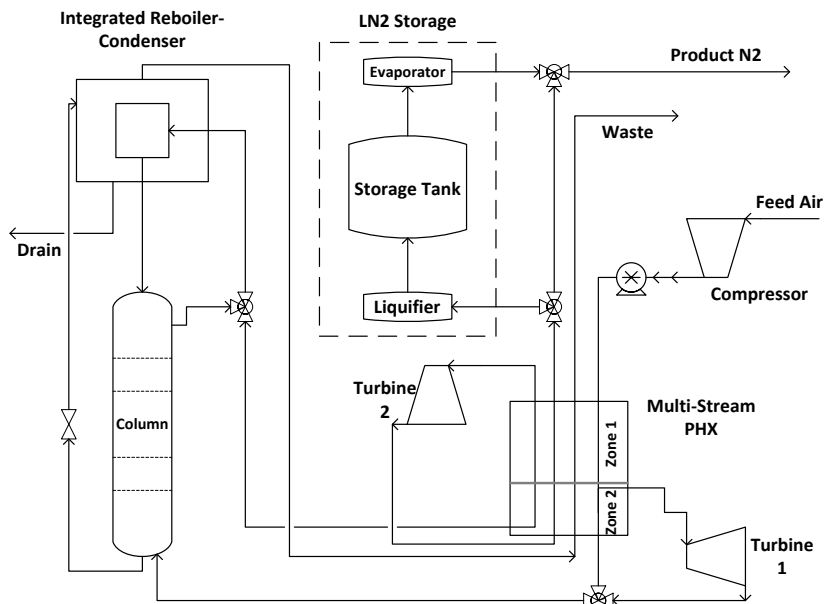


Figure 2: Process flow diagram for the industrial ASU used to generate preliminary operating data, based on Johannsson [6].

The cryogenic column produces high-purity nitrogen gas, which is delivered via pipeline to industrial users. The inlet feed air stream is compressed from ambient pressure to 6.8 bar; the compressor is the main electricity consumer in the process. This consumption is partially offset by the power supplied by the two turbines, which are assumed to be connected to generators. Following the compressor, the air enters the primary multi-stream heat exchanger (PHX), where it condenses and is fed to the bottom of the cryogenic distillation column. A near-pure (with parts-per-million (ppm) levels of oxygen impurity) nitrogen gas stream is obtained at the top of the distillation column. The nitrogen stream passes through the PHX, where it partially provides refrigeration for the feed stream, before it is directed either to the users or to the storage system

where it is liquefied. The storage tank after the liquefier is modeled as a simple integrator. We refer the reader to our work [7] for a complete description of the plant and associated model equations.

Task 2.2 Industrial data collection

Industrial data (Figure 3) were collected from a facility producing nitrogen, oxygen, and argon, whose operation was subject to fluctuations in production due to, e.g. demand or changes in local electricity prices. These fluctuations were likely imposed by operators based on heuristic arguments. The data were recorded at one-minute intervals in the model predictive control system and process historian database, during periods of regular, unforced operation. Periods of start-up, shut-down, and process or measurement faults were excluded. These periods were identified easily in the historical data, as the sensors are either off or produce readings that are, e.g., outside the physical bounds for the respective variables. Although shut-downs of the entire ASU could potentially be scheduled to avoid consuming electricity during price peaks, they were not considered here. However, the shutdown of the liquefier unit was considered.

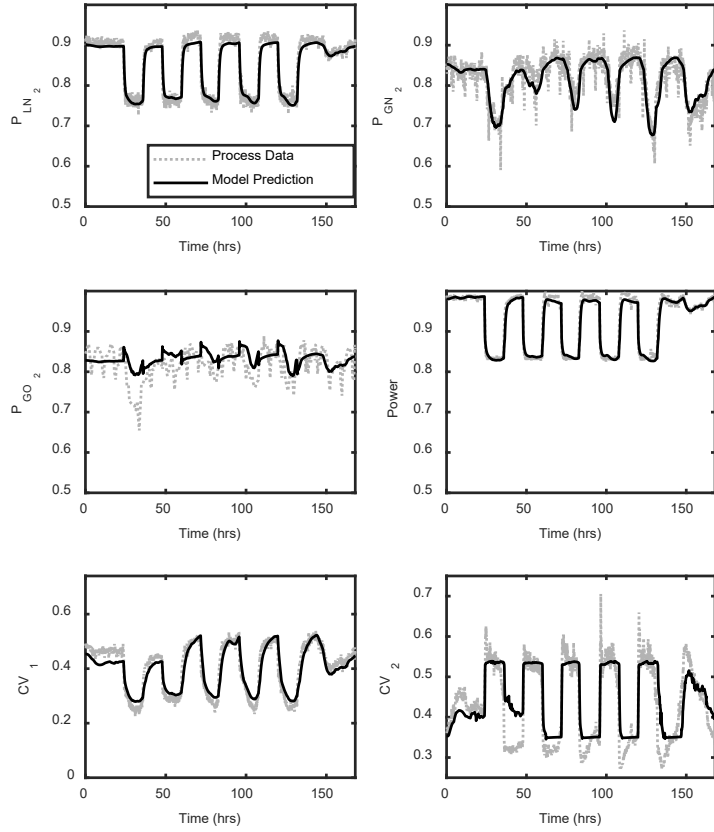


Figure 3: Historical data from industrial process and preliminary data-driven model predictions from [8].

Task 2.3 Model variable selection.

Physical arguments (e.g., proximity to operating constraints) as well as data-driven selection techniques (e.g., variable importance in projection) were considered in building a selection algorithm for the variables used in constructing a DR scheduling-relevant dynamic model. Scheduling-relevant variables were defined as variables that were at or near their operating constraints during normal operation or were directly used to calculate

the operating cost of the ASU. In our work [7], we defined 8 scheduling-relevant variables for the model single-product ASU, presented in Table 1.

Table 1: Summary of scheduling-relevant variables and their rationale, from [7].

Variable	Rationale
Production rate, F^P	Objective function; $16 \leq F^P \leq 24$ (mol/s)
Feed flowrate, F^f	Objective function
Impurity level, I^P	$I^P \leq 2000$ ppm (1800 ppm backoff)
Temperature difference, ΔT	$T_{\text{condenser}}^{\text{o}} - T_{\text{reboiler}}^{\text{o}} \geq 1.8$ °C (2 °C backoff)
Zone 1 pressure ratio, P^d	$P^d \leq 0.96$ (0.95 backoff)
Max flooding fraction, δ^f	$\delta^f \leq 0.97$ (0.96 backoff)
Reboiler holdup, M^R	$0 \leq M^R \leq 150$ kmol; $M^R(0) \leq M^R(N_I T_I)$
Storage holdup, s	$0 \leq s \leq 200$ kmol ; $s(0) \leq s(N_I T_I)$
Production rate, F^P	Objective function; $16 \leq F^P \leq 24$ (mol/s)

Task 3.0 Low-order Dynamic Model Identification.

The purpose of production scheduling for DR operation is to maximize profit (derived from operating under time-sensitive electricity prices), while, (i) meeting product demand, (ii) abiding by all process constraints, related to e.g., product quality and safety and (iii) accounting for the process dynamics. In the context of chemical process operations, DR scheduling is part of a hierarchical decision-making structure that also includes process control, as illustrated in Figure 2. As mentioned in the introduction, one of the challenges of obtaining a computationally-efficient DR scheduling calculation, amenable to real-time solution, is the complexity of the process model, which is manifest in its nonlinearity and high dimensionality. This issue is exacerbated by the disparity between time horizons of DR scheduling, process control and the dynamics of the process itself, meaning that the time horizon of DR scheduling typically spans multiple days (as explained later), and the process dynamics must be considered explicitly over this entire time interval.

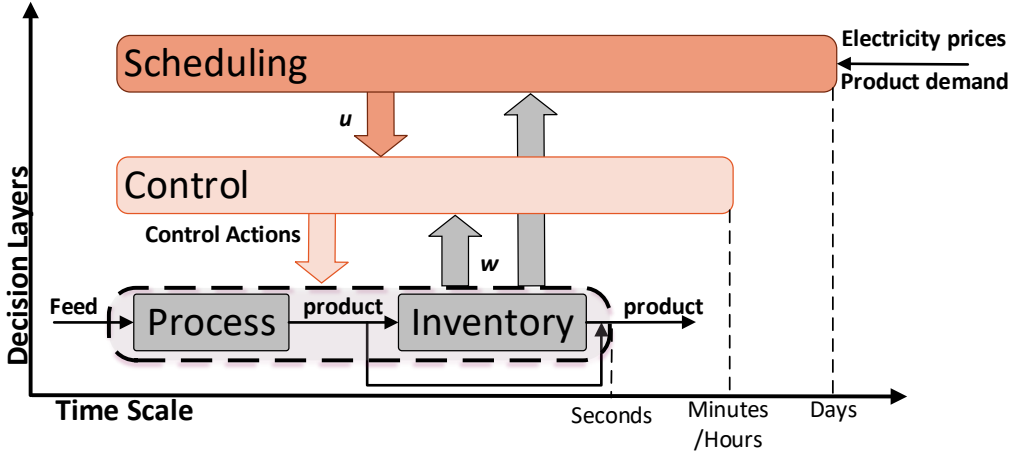


Figure 4: Hierarchy of decisions for chemical process operation, where u are the production set-points/targets and w are the values of the process variables.

A potential approach to deal with these computational challenges lies in representing the plant dynamics using a low-order model. This is not necessarily a new approach conceptually speaking; the novelty of our work consists in identifying which variables are relevant for DR scheduling (and whose dynamics should therefore be modeled), and on introducing the concept of Scale-Bridging Models (SBMs), as a representation of the *closed-loop dynamics* of these variables – that is, SBMs capture the dynamic of the process and its control system (Figure 2), as they respond to target signals generated at the scheduling level. We note that “scale bridging” thus refers to the fact that these models bridge the (fast) time scale of the process with the (longer) time scale of scheduling calculations. We elaborate below.

Task 3.1 Nonlinear model identification.

We considered two classes of low-order models as candidate structures for deriving SBMs: finite step response (FSR) and Hammerstein Wiener (HW), and compare the ability of such models to reproduce (and predict) the behavior of chemical processes. For the simulated problem (Task 2.1), FSR models were fitted for two scheduling-relevant variables: the production rate, and the feed flowrate (Table 3). HW models were fit to the remainder of the scheduling-relevant variables listed in Table 1. The form of the HW model is given below in Figure 3, where a linear state-space model is surrounded at the input/output by static nonlinear functions (e.g. polynomials or piecewise linear functions), the fit of the HW models is given in Table 2.



Figure 5: HW model form, from [7].

For a full discussion of HW and FSR models, we refer the reader to our published works [7], [9].

Table 2: Summary of model fits for the HW models from [7].

Input	Output	Input Nonlinearity		Linear Dynamics		Output Nonlinearity		NMSE	
		u	w	$H(u)$ Breakpoints	State-space Order	$W(y)$ Type	$W(y)$ Breakpoints	Training	Validation
\underline{F}^p	I^p			4	4	PWL	6	0.82	0.52
\underline{F}^p	M^R			3	4	linear	--	0.78	0.75
\underline{F}^p	δ^f			5	5	quadratic	--	0.91	0.92
\underline{F}^p	P^d			2	8	quadratic	--	0.83	0.97
\underline{F}^p	ΔT			9	4	PWL	6	0.69	0.84

Table 3: Summary of model fits for the FSR models from [7].

Input u	Variable	Sample Time (mins)	NMSE	
			Training	Validation
\underline{F}^p	F^p	1	5.1E-08	6.4E-08
\underline{F}^p	F^f	1	3.9E-08	4.3E-08

Task 3.2 Model linearization.

We note that the HW models are nonlinear; embedding them in a schedule optimization calculation results in a nonlinear optimization problem, which poses specific solution challenges in terms of, among others, solution time and global optimality guarantees. It is advantageous to formulate scheduling problems as (mixed integer) linear programs. To this end, the nonlinear input and output functions in the HW models can be linearized. For the cases that we considered in our work, we utilized piecewise linear functions for the Hammerstein and Wiener blocks, and demonstrated that these functions can be linearized exactly as a set of linear expressions comprising a integer and continuous variables. For a comparison of linearization methods, please see our work [9]. Table 4 shows the percent fit between the linearized HW models and the nonlinear continuous HW models. Since the SOS2 linearization is exact, the slight errors in fit are a result of the discretization of the continuous HW models.

Table 4: Model statistics for linearized HW models.

Variable	Sample Time (mins)	%Fit

I^P	6	99.85
M^R	0.5	99.93
dT	6	99.80
δ^f	10	99.63
P^d	10	99.97

Task 4.0 DR Scheduling Problem Formulation and Solution

The above (full order and reduced-order) representations of the ASU were used to formulate and solve multiple scheduling problems. We discuss these problems below based on the objective function and type of knowledge assumed (certain/uncertain).

1. DR scheduling assuming perfect price and demand knowledge.

The problems are compared in terms of model type and solution time. In all cases, the decision variable is the hourly setpoint for production rate, \bar{F}^p .

- a. Optimization problem formulated using the full-order first principles model (DR1). This problem is a nonlinear dynamic optimization problem.

$$\min_{\bar{F}^p(t)} J = \int_0^{T_m} Price(t) Power(t) dt$$

s.t. Timing constraints
 Process model (Full-order)
 Inventory model
 Initial Conditions
 Process and Quality Constraints

- b. Optimization problem formulated nonlinear continuous HW models (DR2). This problem is a nonlinear dynamic optimization problem.

$$\min_{\bar{F}^p(t)} \phi = \int_0^{T_m} Price(t) Power(t) dt$$

s.t. Timing constraints
 Process model (HW)
 Inventory model
 Initial Conditions
 Process and Quality Constraints

- c. Linearized and discretized HW/FSR models (DR3). This problem is a mixed-integer linear program.

$$\min_{\bar{F}^p} Cost = \sum_i \sum_j Price_i Power_{ij}$$

s.t. Timing constraints

Process model (HW/FSR)
 Inventory model
 Initial Conditions
 Process and Quality Constraints
 Continuity Constraints

d. Linearized and discretized HW/FSR models with Lagrangian Relaxation (LR) (DR4). This problem is a mixed-integer linear program.

$$\begin{aligned}
 \min_{\overline{Fp}} J = & \sum_i \sum_j Price_i \mathcal{P}ower_{ij} - \sum_{i=2}^{N_i} \sum_{k=1}^n \lambda_i^k |x_{i-1, N_j}^k - x_{i, j=1}^k| \\
 \text{s.t.} & \text{Timing constraints} \\
 & \text{Process model (HW/FSR)} \\
 & \text{Inventory model} \\
 & \text{Initial Conditions} \\
 & \text{Process and Quality Constraints} \\
 & x_{i,j} \in \mathcal{D}_x \subset \mathbb{R}^n \forall i \forall j
 \end{aligned}$$

e. Rate of change (ROC) representation of ASU (DR5). This problem is meant to reflect the current practice for DR scheduling, where the process dynamics are not represented explicitly but rather in the form of rate of change/ramp rate limits/constraints.

$$\begin{aligned}
 \min_{\overline{Fp}} J = & \sum_i \sum_j Price_i \mathcal{P}i_{ij} \\
 \text{s.t.} & \text{Steady-state gain model} \\
 & \text{Inventory model} \\
 & \text{Initial Conditions} \\
 & \text{Process and Quality Constraints} \\
 & \text{Rate of change constraints}
 \end{aligned}$$

DR1-DR5 all seek to minimize the operating cost of the ASU, which is a function of the time-varying power consumption and hourly electricity prices. DR1 utilizes the full-order first-principles model derived in [6] to represent the ASU. DR2 uses HW models to represent all scheduling-relevant variables (Table 1), and a continuous time-vector. DR3 utilizes HW models for all but two scheduling-relevant variables, which are modeled using FSR models. The HW models in DR3 were linearized with SOS2 and all FSR/HW models were discretized. The problem structure of DR3 is given in Figure 4, where discrete subproblems representing each hour in the time horizon are spanned by an overarching common problem, summing over all subproblems. Each subproblem is linked by a continuity constraint, where states at the end of the previous hour must be equal to the states at the start of the current hour. The subscript i represents each hourly time slot considered in the scheduling calculation, while subscript j corresponds to the discretization time step of the dynamics of the process (typically one minute).

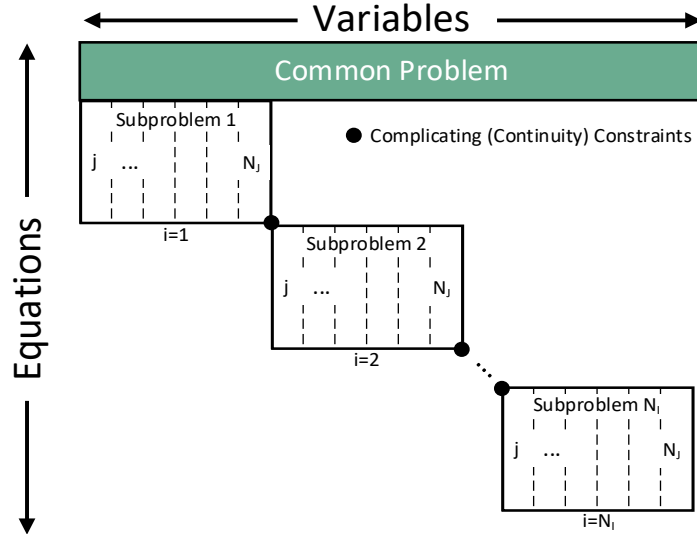


Figure 6: Problem structure for DR3.

For DR4, we produced a new Lagrangian Relaxation strategy (LR), which “unlinks” the subproblems identified based on analyzing the structure of DR3, and enables parallel solution of the scheduling problem. In LR, the complicating (equality) constraints are dualized and penalized in the objective function, leading to the objective seen in DR4. The DR4 objective is the operating cost plus the constraint violations, which in effect, minimizes the operating cost and the continuity violations. Specifically, the difference between states at the end of a scheduling slot and the states at the start of the subsequent slot ($|x_{i-1, N_j}^k - x_{i, j=1}^k|$) is multiplied by a penalty multiplier (λ_i^k), for which there are many selection metrics, covered in detail in [7], [9]. For linear or convex problems, global optimality of the solution to the LR problem can be proved, wherein the constraint violations go to zero and the objectives of DR3 and DR4 are equivalent [7], [9].

Lastly, the ROC problem in DR5 was used as a comparison to more naïve scheduling methods, where a steady-state gain model represents the relationship between production rate setpoint, $\overline{F^p}$, and plant production rate, with the ROC of setpoints between hours limited to be less than 0.5mol/s [7].

Table 5: Summary of results for the 3-day DR scheduling problem of an ASU when optimal schedules for DR2-DR5 were simulated on the full-order model of the ASU. *ROC solution had several constraint violations [7]. The constant production rate represents the base case where DR scheduling is not performed. Savings are calculated relative to the operating cost of this case.

Problem	Model	Cost (\$)	Savings (%)	CPU (h)	Type
DR1	Full-Order	1012.56	1.22	>100	NLP
DR2	Nonlinear HW	1014.68	1.01	5.10	MINLP
DR3	Discrete HW/FSR	1013.64	1.12	0.119	MILP
DR4	Discrete HW/FSR+LR	1013.64	1.12	0.195	MILP
DR5*	ROC	1021.49*	0.35	1.25E-4	LP

Constant Prod. Rate	--	1025.09	--	--	--
---------------------	----	---------	----	----	----

The numerical results for the 3-day scheduling problem in [7] are shown in Table 5, where the full-order model had the lowest objective function but a solution time far too large to be valuable (i.e., the result for three days – 72 hours) – of operation were obtained in more than 100 hours). The linearization and discretization of the HW models and the introduction of FSR models significantly reduced the computation time and achieved a comparable objective function value.

A second set of scheduling problems followed an environmental objective, that is, we investigated the effect of grid-side emissions (due to time-varying contribution of renewables to generation mix) on DR scheduling. Emissions related to power generation do follow a similar profile to electricity prices, in the sense the relative contribution of renewables increases at night (wind) and during mid-day (solar), while fossil-based power generation is used to satisfy power demand during the late afternoon peaks. We define an aggregate emissions metric (CO2 equivalent emitted / kWh generate) which we use in the objective function to minimize emissions related to plant operations. The relevant scheduling problems are described below.

2. Scheduling assuming perfect price, grid-side emissions, and demand knowledge [10]. The decision variable is the hourly setpoint for production rate, \bar{F}^p .

a. Emissions-minimizing production (EMP)

$$\min_{F_i^p} G = \sum_i \sum_j \text{Power}_{ij} \text{Emissions}_i$$

s.t. Timing constraints

Process model (HW/FSR)

Inventory model

Initial Conditions

Process and Quality Constraints

Continuity Constraints

b. DR (equivalent to DR3 above)

$$\min_{\bar{u}_i} J = \sum_i \sum_j \text{Power}_{ij} \text{Price}_i$$

s.t. Timing constraints

Process model (HW/FSR)

Inventory model

Initial Conditions

Process and Quality Constraints

Continuity Constraints

The EMP and DR problems were solved for three or four 3-day periods within each month of 2017 and compared to a reference problem, where the production rate was kept constant. Data for emissions and prices were collected for a CAISO node in Fresno, CA. Figure 5 shows the mean emissions and operating cost across the 3-day periods examined for each month of 2017. It was found that DR, which minimizes operating cost, consistently reduces emissions when compared

to the reference problem (up to 3.36%) and that EMP, which minimizes emissions, has the potential to increase operating cost compared to the reference problem (by up to 7.88%).

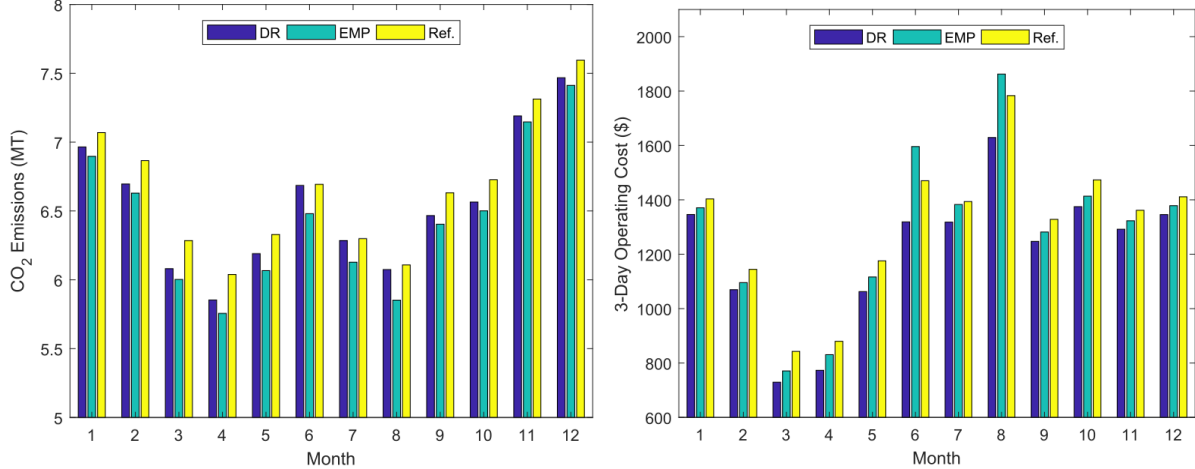


Figure 7: 3-day emissions and operating cost for EMP, DR, and the reference problem (without DR) from [10].

Subsequently, we addressed the (realistic) question of dealing with uncertainty in forecasts of electricity prices (beyond the 24h period for which day-ahead prices can be safely assumed to be known) in the DR scheduling problems. This third set of results is described below.

3. The third set of scheduling problems utilizes chance constraints to represent electricity price and product demand uncertainty. We solve four scheduling problems and compare them in terms of objective function value at the optimum and robustness benefit, for the full results please see [1].

a. Deterministic scheduling problem (equivalent to DR3) (CC1)

$$\min C = \sum_i \sum_j Price_i Power_{i,j}$$

s.t. Process model (HW/FSR)

Process constraints

Quality constraints

Initial conditions

Continuity conditions

Demand constraints ($D = 20 \text{ mol/s}$)

b. Price uncertainty (CC2)

$$\min C$$

$$\text{s.t. } C + (1 - z_r^P)M \geq \sum_i \sum_j Price_{i,r} Power_{i,j}$$

$$\sum_r z_r^P \pi_r \geq \alpha$$

$$\pi_r = \Pr[P_{i,r}]$$

$$0 < \alpha \leq 1$$

$$P_i \sim \mathcal{N}_{mvn}(\mu_i, \Sigma_i)$$

Process model (HW/FSR)

Process constraints

Quality constraints
 Initial conditions
 Continuity conditions
 Demand constraints ($D_i=20$ mol/s)

c. Demand uncertainty (CC3)

$$\min C = \sum_i \sum_j Price_i Power_{i,j}$$

$$\text{s.t. } F_{i,j}^p - D_{i,r} \geq f_{s_{i,j}}^{in} - f_{s_{i,j}}^{out} - M(1 - z_r^D)$$

$$\sum_r z_r^D \geq \alpha N_R^D$$

$$0 \leq \alpha \leq 1$$

$$D_i \sim \mathcal{U}[16,23] \quad t_{start} \sim \mathcal{U}[0,72]$$

Process model (HW/FSR)

Process constraints

Quality constraints

Initial conditions

Continuity conditions

d. Price and demand uncertainty (CC4)

$$\min C$$

$$\text{s.t. } C + (1 - z_r^P)M \geq \sum_i \sum_j Price_{i,r} Power_{i,j}$$

$$\sum_r z_r^P \pi_r \geq \alpha$$

$$\pi_r = \Pr[P_{i,r}]$$

$$F_{i,j}^p - D_{i,r} \geq f_{s_{i,j}}^{in} - f_{s_{i,j}}^{out} - M(1 - z_r^D)$$

$$\sum_r z_r^D \geq \alpha N_R^D$$

$$0 \leq \alpha \leq 1$$

$$D_i \sim \mathcal{U}[16,23]$$

$$P_i \sim \mathcal{N}_{mvn}(\mu_i, \Sigma_i)$$

Process model (HW/FSR)

Process and quality constraints

Initial conditions

Continuity conditions

For CC2-CC4, chance constraints were used to represent the uncertainty. Chance constraints ensure that the probability of meeting the constraint containing the uncertain parameter is above some specified tolerance, α . We utilized binary variable, z , to denote whether the uncertain constraint was met, for demand ($z_r^D \forall r = 1 \dots N^D$) and for price ($z_r^P \forall r = 1 \dots N^P$) uncertainty. If a constraint r was met, $z_r=1$, otherwise, $z_r=0$. For price uncertainty, the number of pricing

scenarios considered was $N^P = 200$. For demand uncertainty, $N^D = 20$ samples were considered. The probability of each price scenario, $Price_{i,r} \forall i = 1 \dots 72$, occurring is π_r , where $\sum_r \pi_r = 1$. Since demand was drawn from a uniform distribution (each scenario has equal probability of occurring), the probability of each scenario is $\frac{1}{N^D}$. For a full discussion of the formulations of CC2-CC4, please refer to our work, [1].

Figure 9 shows that the chance-constrained problem, CC2, has the lowest mean operating cost compared to the two methods which don't consider electricity price uncertainty.

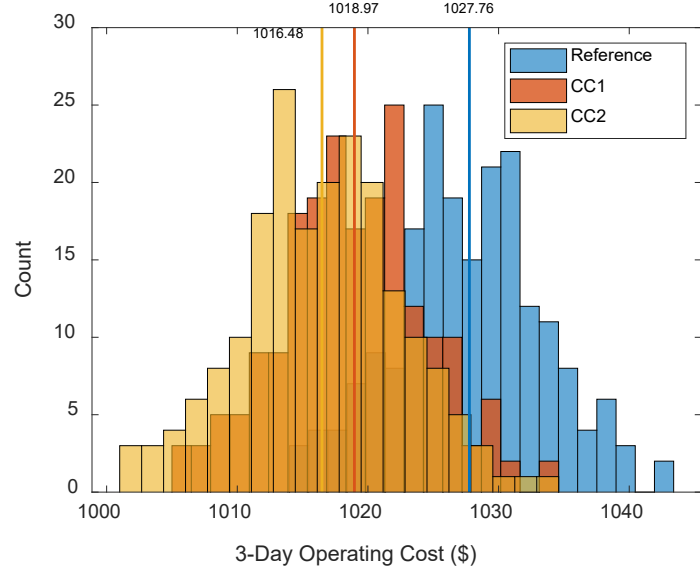


Figure 8: Histogram of the simulated operating cost across all scenarios for CC1-CC2 and the reference problem (no DR), with labeled vertical lines representing the mean values from [1].

In the interest of ensuring feasibility when considering scheduling under demand uncertainty, we assumed that product can be purchased from a competitor at a high premium, when it is not available locally (either from current production or from the storage tank). This penalty is reflected in the operating cost in scenarios where the simulated optimal schedule of CC1 and the reference schedule led to storage depletion and an inability to meet demand, and can be seen in Figure 10 in the bi-modal distributions for the reference and CC1 operating costs (9). While the mean operating cost of the deterministic problem, CC1, is the lowest, the potential for a significantly greater cost is evident, therefore, the risk of not considering uncertainty is high.

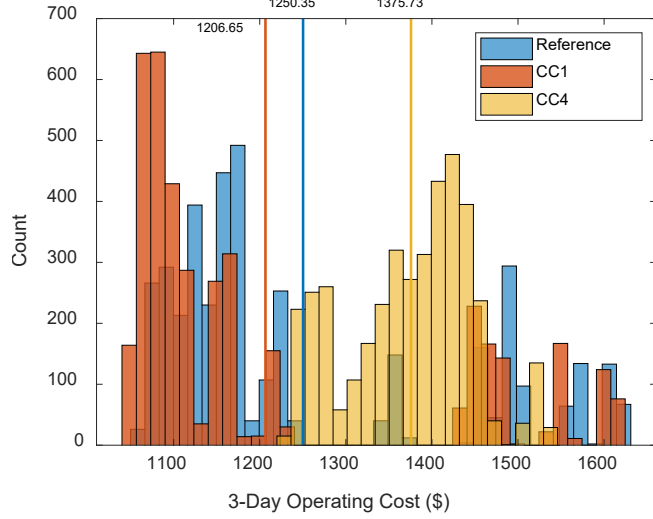


Figure 9: Histogram of the simulated operating cost across all scenarios for CC1, CC4, and the reference problem (no DR), with labeled vertical lines representing the mean values from [1].

The final metric we use to compare scheduling methods is the energy benefit for the subsequent scheduling time horizon (meaning, if the scheduling process were to be continued for subsequent times in the future), which arises from any material available in storage at the end of the time horizon *in excess of* the initial storage level. This energy benefit translates to an increased potential for flexible operation in the next time horizon. As shown (Figure 11), the reference case and CC1 both have potential for storage depletion (as evident in the negative energy benefit), compared to the consistently high energy benefit of CC3.

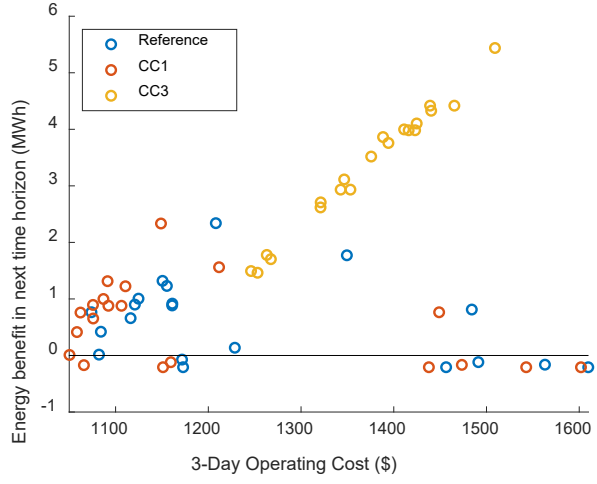


Figure 10: Energy benefit for the next time horizon, where a negative benefit signifies depleted storage, from [1].

4. Another means for dealing with uncertainty in e.g., electricity price and product demand, is rescheduling. We refer to the new method that we proposed as “moving-horizon (MH) scheduling” (in reference to moving horizon optimal control, an advanced control technique). In MH scheduling, deterministic scheduling problems are solved periodically and the solutions are updated once new information becomes available. The problems are

solved on a fixed time horizon, that “shifts” in time (the shift occurs when new information is received). Information updates could include new values for the uncertain variables and/or measurements form the process. Within the MH framework, several different scheduling problems were considered. The examples below use a six-day horizon but the concepts we developed are generic and can be adapted to any time horizon. We refer the reader to our work [11] for more detail. Below we describe the concept behind these MH formulations graphically, rather than relying on mathematical descriptions figures describing the scheduling methods, rather than the scheduling formulations shown in previous sections.

a. Periodic pricing updates

For the case of periodic pricing updates (Figure 10), we consider a scenario where electricity prices are known with certainty for all six days of the time horizon (PP1), a scenario where we only know prices for day one, and use these to estimate the prices on days two and three of the scheduling window (PP2), and a scenario where we assume we have three days of price knowledge at a time. In PP1, we solve the scheduling problem once. In PP2-PP3, we re-solve the problem each day as more prices become available, for a total of four solution cycles (note that this process would continue infinitely as new information arrives). Scenarios PP1-PP3 are a reflection of our ability to forecast electricity prices, and reflect some limit cases: PP2 assumes no forecasting (i.e., reusing prices from one day to forecast prices for all days in the horizon), while PP1 is the opposite case of a fully prescient and accurate price prediction algorithm. We chose to use these limit cases rather than incorporate a price forecasting algorithm in order to fully elucidate the impact of production scheduling on demand response. One can anticipate that the results with a “true” forecasting algorithm would lie between these two limits.

		Scheduling Window	Unscheduled Day	Day in the past
PP1 Ideal				
Reschedule 1		Day 1	Day 2	Day 3
PP2 Realistic				
Reschedule 1		Day 1	Day 1	Day 1
Reschedule 2		Day 1	Day 2	Day 2
Reschedule 3		Day 1	Day 2	Day 3
Reschedule 4		Day 1	Day 2	Day 3
PP3 Less realistic				
Reschedule 1		Day 1	Day 2	Day 3
Reschedule 2		Day 1	Day 2	Day 3
Reschedule 3		Day 1	Day 2	Day 3
Reschedule 4		Day 1	Day 2	Day 3

Figure 11: Scheduling schemes for periodic (daily) pricing updates, where three scheduling methods are considered, from [11].

b. Periodic temperature updates

For the case of periodic temperature updates (Figure 11), we assume temperature predictions become available every 6 hours and consider three scenarios. PT2 considers a scenario where prices and temperatures are known for the entire time horizon, PT3 considers temperature updates every 6 hours on a shrinking horizon

up until the next day begins, where another full day is added to account for new electricity prices, and PT4 maintains a 3-day scheduling window which is shifted forward in time every 6 hours when new temperatures and prices become available.

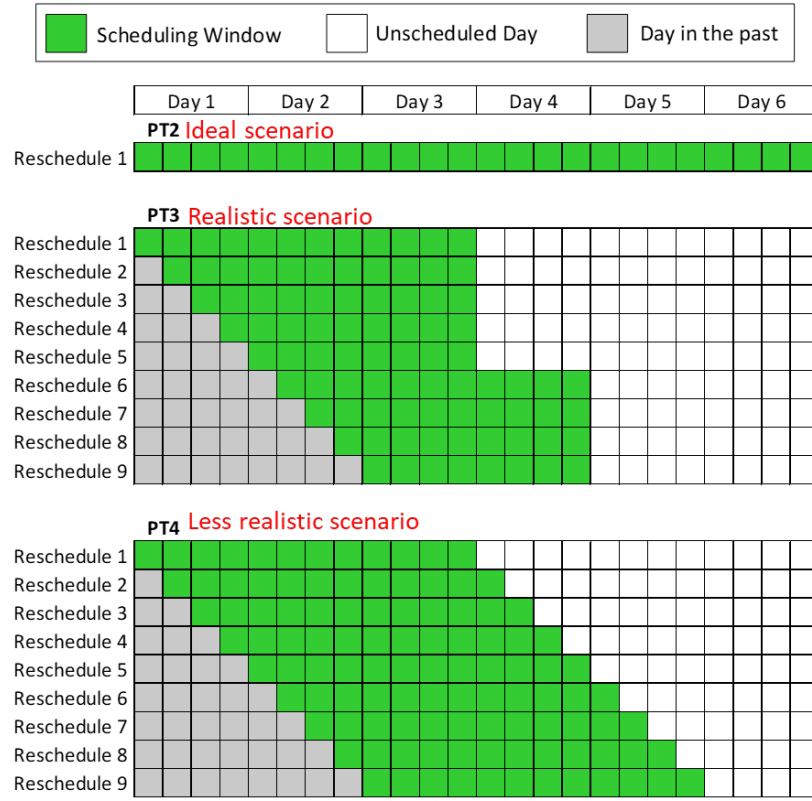


Figure 12: Scheduling schemes for periodic (every 6 hours) temperature updates, where three scheduling methods are considered, from [11].

c. Event-driven rescheduling: product demand (Figure 12)

Lastly, we consider event-driven rescheduling, in the form of demand disturbances. We consider four possible scenarios. PD2 considers planned maintenance, wherein the length and time of the demand disturbance are known, the schedule for PD2 is generated just once. PD3 considers unplanned maintenance, where the start time of the disturbance is unknown but the length is known once it starts, triggering a rescheduling point at the start of the disturbance. PD4 considers a random failure, where neither the start time of the disturbance or the length of the disturbance are known, triggering a rescheduling point at the beginning of the disturbance (where it is assumed the disturbance will carry on throughout the time horizon) and the end of the disturbance. Lastly, PD5 considers the case of random failure, but uses chance constraints to anticipate when the disturbance may end.

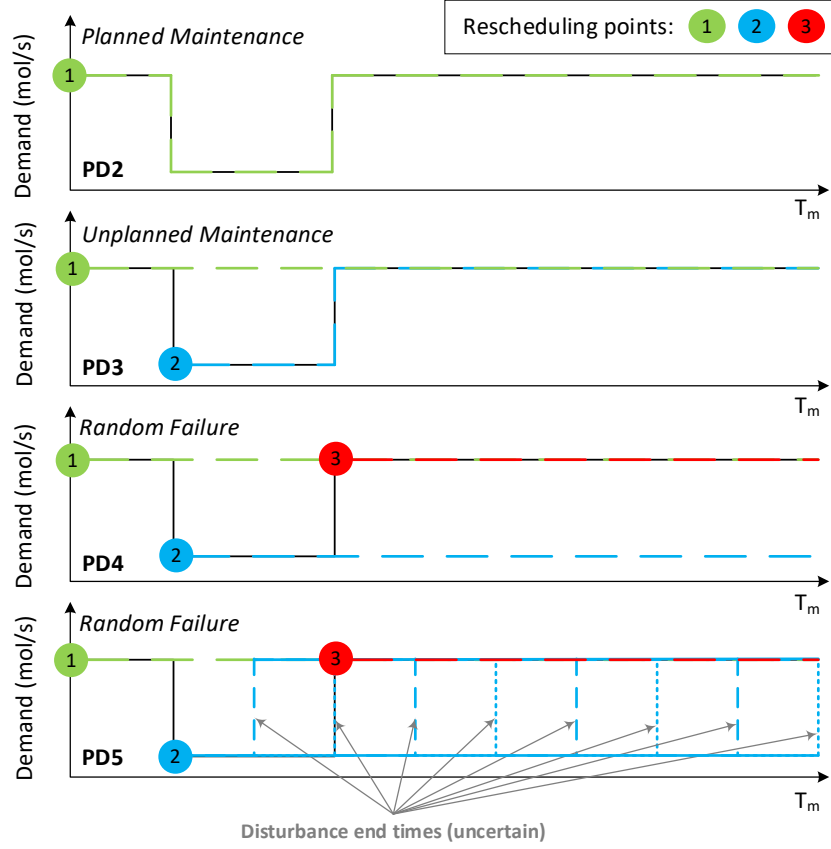


Figure 13: Scheduling schemes for event-driven rescheduling.

For the different scenarios considered, the economics of using a moving horizon rescheduling strategy did not differ significantly from the best case of a scheduling calculation based on perfect knowledge of all disturbances and considering the entire time horizon. This observation is true in the case where moving horizon scheduling itself possesses perfect knowledge of the disturbances for the scheduling window considered. However, even simplistic forecasting strategies for periodic disturbances (e.g., using information from the preceding day) led to economic gains. In terms of event-driven rescheduling, we found that PD4 led to the possibility of depleted storage, but that this shortcoming was remedied by the addition of chance-constraints in PD5. The results from this work are extensive given the number of scheduling schemes provided, so we refer to reader to our published work for a detailed description of the results [11].

Task 5.0 Representation of DR Dynamics of Chemical Processes in Power Systems Models.

Task 5.1 Mathematical modeling

We used a DC approximation of the power grid and aimed to incorporate the chemical process into the grid model for power flow optimization [2]. From the grid perspective, an electricity-intensive chemical process is regarded as a large scale battery and modeled accordingly; we used

a linear model that indicates power consumption limits and storage capacity of chemical products. The transient properties of the grid-connected load (we used a chlor-alkali electrolysis plant as an example) were explicitly represented in the low-order models. Thus, while this modified process model was amenable for use in grid-relevant computations, it also guarantees safe and feasible manipulation of the chemical plant load during DR activities.

We refer to the integrated problem as “cooperative demand response.” For a small-scale grid, incorporating the dynamics of the chemical plant in the optimal power flow calculations results in better resource management leading to up to 15% and 46% cost reduction for the grid and chemical plant operations, respectively, during periods of power line congestion [2]. For the chemical plant, the savings were twice as high as the amount achieved when the chemical plant scheduling is carried out with the chemical plant as a pure “price taker”. Additionally, our simulations reveal that industrial loads can be deployed to achieve smoother DR and correspondingly peak shaving and valley filling at the level of the entire grid.

Task 5.2 Electricity pricing algorithms.

We have developed stochastic programming problems that consider strategies for optimal splitting of electricity purchases in the day-ahead and short term markets [12].

We are currently working on an iterative scheme where the optimal power flow problem is solved at the grid level and the local scheduling problems at the plant level provide additional constraints/feasibility cuts. We expect that this will eventually lead to new pricing/bidding strategies.

IV. Accomplishments and Conclusions

The key objectives stated at the start of this project were:

1. Develop data-driven low-order, DR scheduling-relevant dynamic models of chemical processes:

To this effect, we utilized historical and simulated operating data to derive low-order models of the nonlinear dynamics of chemical plants that are relevant to scheduling their operation for participating in DR programs. We identified SBMs in the form of HW and FSR models for simulated plant data [7] and historical operating data [8]. Concurrently, the formulation and solution of the associated optimal DR production scheduling problems was studied.

2. Develop models and DR scheduling optimization problem formulations that are amenable to real-time solution.

To this effect, we developed a scheduling framework utilizing discretization, linearization, and low-order modeling to represent complex chemical processes. We applied LR to the optimization problem to enable the parallel solution of decoupled subproblems. At the time of publication, we reported a solution time for the 3-day DR scheduling problem of 7.12 minutes [7]. Since then, the solution time for the same problem has reduced to a minute and a half (due to upgrades in optimization solvers and hardware). This fast solution time demonstrates that we have a problem formulation amenable to real-time solution. With this computationally efficient model, we have solved the DR scheduling problem for instances of electricity price uncertainty, product demand uncertainty, and changes in ambient conditions such as temperature [1], [11]. We have also used the scheduling framework to determine the impact of DR on grid-side power generation emissions [10].

3. Create representations of the DR behavior of chemical process that can be embedded in power system models.

Low-order dynamic models for a chlor-alkali process were developed and incorporated into the grid model for power flow optimization [2]. Implementation of this chemical plant model in the optimal power flow calculations resulted in better resource management leading to up to 15% and 46% cost reduction for the grid and chemical plant operations respectively during periods of power line congestion.

We believe we have accomplished the objectives of this project. In order to build a strong foundation for the project, we have several works dedicated to modeling and solving DR optimization problems from the user-side. Our work in preparation begins to look at the problem from the grid-side. We also want to look at networked plants (e.g., air separation units operating on a common pipeline) for DR participation to try and increase the capabilities of industrial DR participants to perform load-shifting. Our considerations of uncertainty in DR have inspired future directions in this area as well: we plan to try multistage methods of optimization under uncertainty to fully investigate the effects of uncertainty (and mitigating this uncertainty) in DR scheduling.

APPENDIX A: Product or Technology Production

Publications:

Kelley, M. T., Baldick, R., & Baldea, M. (2019). Demand Response Operation of Electricity-Intensive Chemical Processes for Reduced Greenhouse Gas Emissions: Application to an Air Separation Unit. *ACS Sustainable Chemistry & Engineering*, 7(2), 1909–1922. Retrieved from <http://pubs.acs.org/doi/10.1021/acssuschemeng.8b03927> OSTI ID: 1615231

Tsay, C., Kumar, A., Flores-Cerrillo, J., & Baldea, M. (2019). Optimal demand response scheduling of an industrial air separation unit using data-driven dynamic models. *Computers and Chemical Engineering*, 126, 22–34. <https://doi.org/10.1016/j.compchemeng.2019.03.022> OSTI ID: 1547602

C Tsay and M Baldea. Integrating production scheduling and process control using latent variable dynamic models. *Control Eng. Pract.*, 2019. (accepted, awaiting publication)

C Tsay and M Baldea. 110th Anniversary: Using data to bridge the time and length scales of process systems. *Ind. Eng. Chem. Res.* 58:16696-16708, 2019. OSTI ID: 1550774

Kelley, M. T., Pattison, R. C., Baldick, R., & Baldea, M. (2018). An efficient MILP framework for integrating nonlinear process dynamics and control in optimal production scheduling calculations. *Computers & Chemical Engineering*, 110, 35–52. <https://doi.org/10.1016/j.compchemeng.2017.11.021> OSTI ID: 1549167

Kelley, M. T., Pattison, R. C., Baldick, R., & Baldea, M. (2018). An MILP framework for optimizing demand response operation of air separation units. *Applied Energy*, 222, 951–966. <https://doi.org/doi.org/10.1016/j.apenergy.2017.12.127> OSTI ID: 1537994

Conference Presentations:

Kelley, M. T., Baldick, R., & Baldea, M. (2019). Greener operation of chemical processes using emissions-based scheduling. In *Texas, Wisconsin, California Control Consortium (TWCCC)*. Austin, TX.

Kelley, M. T., Baldick, R., & Baldea, M. (2018). Green Operation of an Air Separation Unit Using an Efficient MILP Optimal Scheduling Framework. In *American Institute of Chemical Engineers (AIChE) Annual Meeting*. Pittsburgh, PA.

Kelley, M. T., Baldick, R., & Baldea, M. (2019). Demand Response Operation of Electricity-Intensive Chemical Processes for Reduced Greenhouse Gas Emissions: Application to an Air Separation Unit. In *Industrial & Engineering Chemistry Research Student Award Symposium*. San Diego, CA.

Tsay, C., Baldea, M., Shi J., Kumar, A., Flores-Cerrillo, J., (2018). Data-driven models and algorithms for demand response scheduling of air separation units. Texas-Wisconsin-California Control Consortium, Madison, WI.

Tsay, C., Baldea, M., Shi J., Kumar, A., Flores-Cerrillo, J., (2018). Optimal demand response operation of an industrial air separation unit using data-driven, scheduling-relevant dynamic models. AIChE Annual Meeting, Pittsburgh, PA.

Kelley, M. T., Baldick, R., & Baldea, M. (2019). Chance-constrained optimal scheduling of an air separation unit for demand response under uncertainty. In *Computational Science Graduate Fellowship (CSGF) Program Review*. Washington, D.C.

Kelley, M. T., Baldick, R., & Baldea, M. (2019). Proactive (re)scheduling of an air separation unit in demand response scenarios. In *Energy Research Expo*. Austin, TX.

Kelley, M.T., R. Baldick, and M. Baldea, “Green Operation of an Air Separation Unit Using an Efficient MILP Optimal Scheduling Framework,” in *American Institute of Chemical Engineers (AIChE) Annual Meeting*.

Kelley, M.T., R. Baldick, and M. Baldea, “Optimal Production Scheduling for Greenhouse Gas Reduction,” in *McKetta Department of Chemical Engineering 1st/3rd Year Seminar Series*. (10/26/2018)

Kelley, M.T., R. Baldick, and M. Baldea, “Demand Response Operation of Air Separation Units with an Efficient MILP Modeling Framework,” in *DOE Computational Science Graduate Fellowship (CSGF) Annual Program Review*, (7/17/2018).

Kelley, M.T., R. C. Pattison, R. Baldick, and M. Baldea, “Demand Response Operation of Air Separation Units Utilizing an Efficient MILP Modeling Framework,” in *Process Science and Technology Center Meeting*. (04/03/2018)

Kelley, M.T., R. Baldick, and M. Baldea, “Demand Response Operation of Air Separation Units with an Efficient MILP Modeling Framework,” in *UT Austin Energy Week*. (01/29/2018)

Kelley, M.T., “An MILP framework for solving industrial demand response optimal scheduling problems,” in *PhD Candidacy Examination*. (11/30/2017)

Kelley, M.T., Pattison, R. C., Baldick, R., & Baldea, M. (2017). Linear Surrogate Dynamical Models for Embedding Process Dynamics in Optimal Production Scheduling Calculations. In *AIChE Annual Meeting*. Minneapolis. (11/02/2017)

Kelley, M.T., Pattison, R. C., Baldick, R., & Baldea, M. (2017). Demand Response Operation of Air Separation Units Utilizing an Efficient MILP Modeling Framework. In *AIChE Annual Meeting*. Minneapolis. (11/01/2017)

REFERENCES

- [1] M. T. Kelley, R. Baldick, and M. Baldea, “Demand response scheduling under uncertainty: chance-constrained framework and application to an air separation unit,” *AIChE Journal*, under Rev., 2020.
- [2] J. I. Otashu and M. Baldea, “Cooperative demand response based on extended optimal power flow problem,” *Prep.*
- [3] “Daily Renewables Output Data,” Folsom, CA, 2017.
- [4] CAISO, “California Independent System Operator,” 2017. [Online]. Available: <http://www.caiso.com/Pages/default.aspx>.
- [5] ERCOT, “Energy Reliability Council of Texas,” 2017. [Online]. Available: <http://www.ercot.com/>. [Accessed: 03-Apr-2017].
- [6] T. Johansson, “Integrated Scheduling and control of Air Separation Unit Subject to Time-Varying Electricity Price,” KTH Royal Institute of Technology, Stockholm, Sweden, 2015.
- [7] M. T. Kelley, R. C. Pattison, R. Baldick, and M. Baldea, “An MILP framework for optimizing demand response operation of air separation units,” *Appl. Energy*, vol. 222, pp. 951–966, Jul. 2018. OSTI ID: 1537994
- [8] C. Tsay, A. Kumar, J. Flores-Cerrillo, and M. Baldea, “Optimal demand response scheduling of an industrial air separation unit using data-driven dynamic models,” *Comput. Chem. Eng.*, vol. 126, pp. 22–34, 2019. OSTI ID: 1547602
- [9] M. T. Kelley, R. C. Pattison, R. Baldick, and M. Baldea, “An efficient MILP framework for integrating nonlinear process dynamics and control in optimal production scheduling calculations,” *Comput. Chem. Eng.*, vol. 110, pp. 35–52, Feb. 2018. OSTI ID: 1549167
- [10] M. T. Kelley, R. Baldick, and M. Baldea, “Demand Response Operation of Electricity-Intensive Chemical Processes for Reduced Greenhouse Gas Emissions: Application to an Air Separation Unit,” *ACS Sustain. Chem. Eng.*, vol. 7, no. 2, pp. 1909–1922, Jan. 2019. OSTI ID: 1615231
- [11] M. T. Kelley, R. Baldick, and M. Baldea, “An empirical study of moving horizon closed-loop demand response scheduling,” *J. Process Control*, under Rev., 2020.
- [12] J. Simkoff and M. Baldea, “Stochastic scheduling and control using data-driven nonlinear dynamic models: application to demand response operation of a chlor-alkali plant purchasing of electricity,” *Ind. Eng. Chem. Res. Submitt.*